PART III

CHAPTER 10

TRANSMISSION ELECTRON MICROSCOPY - GENERAL INTRODUCTION

CONTENTS

10.1 Introduction

Transmission electron microscopy has now become a well established technique for studying defects in crystals. Some information which can be obtained from an electron optical study is :

1. Burgers vectors and the nature of the dislocation (i.e. separation into partials or not).
2. Stacking faults.
3. Character of dislocations (screw or edge).
4. Poisson's ratio.
5. Stacking fault energies.
6. Surface energy and

7. Location of glide planes in the structure.

TEM technique was developed mainly at the Cavendish laboratory in Cambridge by Hirsch, Whelan, Howie and co-workers[1-3] and independently by Bollmann[4].

Essentially this method involves the preparation of specimens, whose thickness is not more than a few hundred to a thousand angstroms, depending upon the material, and examining them in transmission in the electron microscope operating normally at 120 kV.

Progress in the thinning procedures has been so extensive that it is now possible to prepare specimens suitable for direct transmission electron microscopy with a wide variety of substances. This has resulted in a considerable volume of work being carried out by this technique.

The instrumental resolution of the best electron microscopes is well below 10 Å and sometimes significantly below 1.5 Å, it is common for the resolution in the image to be much poorer than this because the specimen itself limits the resolution. Thick specimens give rise to inelastic scattering of the electrons, which leads to appreciable chromatic aberration effects. Also, the width of the image

features as determined by the a basic electron diffraction contrast mechanisms can be considerably greater than 10 Å.

In considering the application of transmission electron microscopy to the study of crystal defects, first the basic contrast mechanism will be summarised and then the manner in which the contrast theory is applied to the analysis of images will be discussed.

10.2 Image Contrast

There are two important mechanisms which produce image contrast in the electron microscope.

10.2.1 Diffraction contrast

Diffracted electrons leaving the lower surface of a crystalline specimen are intercepted by the objective aperture (Figs. 10.1 and 10.2) and prevented from contributing to the image. Alternatively only one diffracted beam forms the image.

On placing an aperture at the back focal plane of the objective lens of the electron microscope, the aperture allows either the transmitted beam (bright field image (BF)(Fig. 10.3) or the diffracted beam (dark field image (DF)(Fig. 10.4) to

pass through.

10.2.2 Phase contrast

Some of the electrons leaving the specimen are recombined to form the image so that phase differences present at the exit surface of the specimen are converted into intensity difference in the image.

Diffraction contrast is dominant mechanism delineating object detail $\gtrsim 15$ Å in crystalline specimens and is the most important and widely used contrast mechanism for study of crystal defects. Phase contrast is the dominant mechanism for object detail ≤ 10 Å and is important in lattice resolution studies and investigations of the early stages of short-range order in amorphous materials.

10.2.3 Diffraction contrast : summary of theory

Quantitative analysis of crystal defects using the diffraction contrast approach usually involves detailed comparison of BF and DF images. BF images exclude diffracted, and DF images transmitted, electrons. Consequently, they are simply high magnification maps of the intensity distribution

across the transmitted or diffracted beams produced by the interaction of the specimen illuminated with the incident electron beam. Thus image contrast arises from point to point differences in the efficiency of the diffraction process in the region of the specimen under study. As a result, the details of the image must be interpreted in terms of a suitable diffraction theory, which has been described in detail in a number of books[5-10] and review articles[11,12], to which the reader is referred for detailed theoretical background. Here author emphasizes upon the important conclusions of the theory for images of specific types of crystal defect and describes those image features which may be used to characterize the defects under study. Only the basic concepts of diffraction theory are included so that these factors important to the experimentalist may be defined.

Electron microscope images are normally discussed in terms of the dynamical theory of electron diffraction which incorporates as a special case the kinematical theory used to describe electron diffraction patterns. The dynamic theory accurately describes the diffraction process occurring in the electron microscope specimen and has been developed

for the interpretation of image contrast in the electron microscope in a series of papers by Hirsch, Howie, Whelan, Amelinckx, Gevers, Van Landuyt and their co-workers. The details of the theory have been summarised in the books referred to above. The simplest form of the theory only considers the case of two beams - one transmitted through, and one diffracted by the specimen. The following factors not included in the kinematical theory are incorperated in the dynamical theory.

1. The intensity in the diffracted beam may be high compared with the transmitted beam.
2. Electrons may be rediffracted back from the diffracted into the transmitted beam.
3. Absorption of the electrons by the specimen, that is there is a limitation on penetration.

A more detailed formulation of the theory which includes several diffracted beams, the "multi beam" case is summarised in the review articles.[13,14] This is important for accelerating voltages of above 300 kV when two-beam conditions may be difficult to obtain for metallic specimens.

10.2.4 The perfect crystal

The simple two-beam dynamical theory describes the amplitudes ϕ_0 (transmitted) and ϕ_g (diffracted) in an element dz, depth z, in a small column of material in a thin foil thickness t, see Fig. 10.5. This theory assumes the following :

1. The column is narrower than the image but wide enough to contain both the diffracted and transmitted amplitudes. This is possible because the scattering angle for 120 kV electrons is small ($2\theta \lesssim 1^{\circ}$).
2. There is no contribution to the waves in the column from the rest of the specimen and conversely no loss from the column to the specimen.
3. If the crystal is distorted, that is when a crystal defect is present, the distortion occurs down but not across the column.
4. Only plane waves exist in the column.
5. Only one strongly diffracted beam in addition to the transmitted beam exists, that is two-beam condition (Fig. 10.6).

Points (1) - (3) are known as the column

approximation and have been justified in the case of single dislocations[15,16] and for narrow dipoles near the foil surface[17]. Point (5) is more important because it specifies that images to be analysed quantitatively must always be produced under two-beam conditions.

The theory allows for contribution back to the transmitted beam from the diffracted beam. Thus, as the transmitted wave propagates into the crystal, its amplitude ϕ_0 will be depleted by diffraction while the amplitude of ϕ_g is increased correspondingly, that is there is coupling between ϕ_0 and ϕ_g. The coupling is described by a pair of differential equations known as the Darwin-Howie-Whelan equations

$$\frac{d\phi_0}{dz} = \frac{i\pi}{\xi_0}\phi_0 + \frac{i\pi}{\xi_g}\phi_g \exp(2\pi i sz) \qquad 10.1(a)$$

$$\frac{d\phi_g}{dz} = \frac{i\pi}{\xi_0}\phi_0 \exp(-2\pi i sz) + \frac{i\pi}{\xi_g}\phi_g \qquad 10.1(b)$$

where s is the deviation from the exact Bragg angle, (Fig. 10.7) and ξ_0 and ξ_g are constants. The term ξ_g describes a critical distance in the perfect crystal at which the transmitted intensity falls to zero before increasing again and is

known as the extinction distance. The term $\exp(2\pi i sz)$ represents a phase factor arising from the scattering process. The first of these equations states that the change in ϕ_0 in depth dz is partly due to forward scattering by the atoms in the element dz and partly due to scattering from the diffracted beam. Furthermore, there is a phase change of $\pi/2$, represented by the factor i, which arises from the scattering process.

10.2.5 Crystal containing a defect with a strain field

In general, thin electron microscope specimens contain a number of defects such as dislocations, stacking faults, precipitates, etc. Using the case of a dislocation as an example (Fig. 10.8), the equations corresponding to equations (10.1) are

$$\frac{d\phi_0}{dz} = \frac{i\pi}{\zeta_0}\phi_0 + \frac{i\pi}{\zeta_g}\exp(2\pi isz + 2\pi i g.R) \qquad 10.2(a)$$

$$\frac{d\phi_g}{dz} = \frac{i\pi}{\zeta_g}\phi_0 \exp(-2\pi isz - 2\pi i g.R) + \frac{i\pi}{\zeta_g}\phi_g \qquad \ldots \qquad 10.2(b)$$

If the displacement in the column arising from, for example, the strain field of the dislocation at DD in Fig. 10.8 is R(Z). In these equations all symbols have the same meaning as in equation 10.1 and 'g' is the reciprocal lattice vector for the operative reflecting plane. Effectively these equations mean that the distortion of the lattice causes a phase factor $\exp(-i\alpha)$, where $\alpha = 2\pi g.R$, to be superimposed on the normal scattering process for the perfect crystal. If the atom is displaced by R, the phase of the scattered wave is changed by $\exp(-2\pi g.R)$. Since this phase factor in equation 10.2(a) describes scattering from diffracted to transmitted beam as $\exp(+2\pi g.R)$ for the reverse process it is $\exp(-2\pi g.R)$ in equation 10.2(b). Thus, when one forms a BF image of a distorted crystal in the electron microscope by excluding the diffracted electrons with the objective aperture, one obtains a bright field image with some dark regions arising from the enhanced diffraction by the strain field of the crystal defects.

The physical significance of equation 10.2 may be made clear as follows.

Substituting

$$\phi_g' = \phi_g(z) \exp(-\pi i z/\xi_o) \text{ and}$$

$$\phi'_g = \phi_g(z) \exp\left(2\pi i s z - \frac{\pi i z}{\zeta_0} + 2\pi i \mathbf{g}.\mathbf{R}\right)$$

in equation 10.2 leads to

$$\frac{d\phi'_0}{dz} = \frac{\pi i}{\zeta_g} \phi'_g \qquad .. \qquad .. \qquad 10.3(a)$$

$$\frac{d\phi'_g}{dz} = \frac{\pi i}{\zeta_g} \phi'_0 + \left(2\pi i s + 2\pi i \mathbf{g}.\frac{d\mathbf{R}}{dz}\right) \phi'_g \qquad 10.3(b)$$

Thus the strain field of the dislocation enters the equation as $\mathbf{g}.\left(\frac{d\mathbf{R}}{dz}\right)$ and acts like a local rotation of the reflecting planes which changes the value of s. Consequently the local diffracted intensity can be considered to increase because the local Ewald sphere construction passes nearer the s = 0 position in reciprocal space (Fig. 10.7).

Of course, the above approach also enables strain-free situations to be described in which the phase factor α arises from the simple displacement of one part of the crystal relative to another, by a vector R , such as occurs in the case of stacking faults.

Note that the characteristic features

of a perfect crystal will also be present but the details may be destroyed if a high density of crystal defects is present.

10.2.6 Experimental conditions for quantitative analysis

1. Images should always be produced under two-beam dynamical conditions so that the preceding theory may be quantitatively applied.
2. In BF images deviation from the Bragg position, s should be small and positive (bright Kikuchi line just outside diffraction spot, see Fig. 10.9). Under these conditions both better transmission and sharper clearer contrast are obtained than at s = 0 or negative.
3. In dark field the deviation from the Bragg position may be upto $\pm$ 1 but, if comparison is to be made with bright field images, specific values of w may be required depending on the case under consideration.
4. Thin areas $< 2 - 3\xi_g$ should be avoided because significant rearrangement of mobile crystal defects occurs[7] particularly if the

friction stress on dislocations is low.

5. Regions of rapidly changing thickness should be avoided if the detailed image contrast is to be studied because of the marked changes in background intensity produced by thickness fringes.

6. The most suitable specimen thickness for observation at 120 kV under all reflections are those $5 - 8\ \xi_g$ thick, where ξ_g is the extinction distance of a low index reflection.

7. Where maximum penetration is important, careful selection of the operative reflection is essential because penetration depends upon the operative reflection even in pure metals. For example in hexagonal metals $\{2\bar{2}00\}$-type reflections are more intense and give better penetration than $\{1\bar{1}00\}$- type reflections.

Author now proceeds to consider some samples for contrast at imperfections.

10.3 <u>Stacking Faults</u>

This is the simplest type of planar imperfection. The crystal below the fault is identical

to that above the fault in spacing and in orientation but is translated with respect to it by some constant vector $\vec{R}$ (Fig. 10.10). The phase factor α determining the contrast thus changes abruptly from zero above the fault to the value $\alpha = 2\pi\vec{g}.\vec{R}$ below the fault. This formula gives the necessary result that if $\vec{R}$ is a lattice translational vector, this means that the two crystals are once more in perfect register, the fault is invisible for all reflections $\vec{g}$ since α merely changes from zero to the equivalent value of $2n\pi$, where n is an integer.

If R is not a lattice translational vector, however, there may be particular values of $\vec{g}$ for which $\vec{g}.\vec{R}$ takes integral values. An important technique in the study of stacking fault is therefore to identify the reflections in which the fault is invisible. With sufficient information of this type, the displacement vector $\vec{R}$ can be determined. Of course, if the value of $\vec{g}.\vec{R}$ is very close to an integer the fault may be effectively invisible, this if found true in practice if $\vec{g}.\vec{R}$ differs from an integer by less than about 0.02.

10.4 Quantitative Analysis of Crystal Defects Using Diffraction Contrast

10.4.1 Dislocations - A simple treatment of dislocation images

The image may be calculated using equations 10.2 and depends upon the operative reflection $\vec{g}$, the deviation s from the Bragg position and the displacement field $\vec{R}$ of the dislocation. The latter depends upon the dislocation line direction $\vec{u}$, the Burgers vector $\vec{b}$, orientation within the thin foil and the elastic anisotropy of the material. However, initially the case of elastically isotropic material is used to describe qualitatively the useful features of the image.

Consider the simple case in Fig. 10.8 in which a straight screw dislocation Burgers vector $\vec{b}$ lies parallel to the surface of a thin foil at a depth y. The displacement $\vec{R}$ of the atoms in the element dz of the column defined relative to the dislocation core by the coordinate r and the angle β is given, for an infinite elastically isotropic material, as

$$\vec{R} = \frac{\vec{b}\beta}{2\pi} \qquad .. \qquad .. \qquad 10.4$$

Thus α to be inserted in equation 10.2 is

$$\alpha = \vec{g}.\vec{b}\beta$$

Clearly the form of the dislocation image depends directly upon the term $\vec{g}.\vec{b}$ which may be either zero or an integer for a perfect dislocation, because it is a scalar product of a real lattice vector with that of a reciprocal lattice. However, for a partial dislocation for which $\vec{b}$ is a fractional lattice vector, $\vec{g}.\vec{b}$ may be zero, a fraction or an integer.

For perfect or partial dislocations with $\vec{g}.\vec{b}$ = 1, 2, etc., the image is a dark line in BF arising from the finite value of α in equation 10.2(a). For partial dislocations with fractional values of $\vec{g}.\vec{b}$, the contrast is complicated. However, the single most useful feature of dislocation images is the invisibility of dislocations in BF and DF images when $\vec{g}.\vec{b}$ = 0. In this situation equation 10.2(a) is identical with equation 10.1(a) that is the crystal behaves as if the dislocations were not present. It is this property of the electron microscope image of dislocations, known as the "$\vec{g}.\vec{b}$ = 0 invisibility criterion" which enables the direction of the Burgers vector of a dislocation to be obtained.

As pointed out in section 10.2.5 with

equation 10.3, the dislocation image may be considered in terms of the distortion of the reflecting planes. The $\vec{g}.\vec{b} = 0$ situation corresponds to the case when $\vec{b}$ lies in the reflecting plane, (Fig. 10.8(b)). Here an edge dislocation lies parallel to the surface of a thin foil with $\vec{b}$ parallel to the foil normal. The solid lines correspond to a set of distorted planes but the dashed lines are, to a first approximation, undistorted planes because they contain $\vec{b}$. Thus, as far as diffracted and transmitted electrons are concerned, the crystal is not distorted, that is it behaves as if the dislocations were not present. However, if the reflecting plane does not contain $\vec{b}$, as shown in Fig. 10.8(c), the reflecting planes shown as dashed lines are distorted. Thus if the angle of incidence of the electrons is $\theta + \Delta\theta$ in the undistorted specimen far from the dislocation (that is everywhere else in the specimen) s will be positive and there will be a high intensity everywhere in the BF image because s positive corresponds to a low diffracted intensity (Fig. 10.7), that is high transmitted intensity. However, near the dislocation the reflecting planes are distorted towards s = 0 when the diffracted intensity increases, that is transmitted intensity will be reduced (Fig. 10.7) and the dislocation

is visible as a dark line on a bright background in BF.

10.4.2 Partial dislocations

The contrast effect at partials can be understood based on the principle given in the previous two sections. In the case of partial dislocations the product $\vec{g}.\vec{b}$ is no longer an integer. In the face centred cubic system Sheckley partial dislocations are of the type.

$\vec{b} = \frac{a}{6}[2\,11]$ and $\vec{g}.\vec{b}$ can take the values $0, \pm\frac{1}{3}, \pm\frac{2}{3}, \pm 1, \pm\frac{4}{3}$, etc. Kinematical (as also the dynamical) calculations show that screw dislocations with $\vec{g}.\vec{b} = \frac{1}{3}$ are invisible, but those with $\vec{g}.\vec{b} = \frac{2}{3}$ are visible[18]. It should be noted, however, that more recent calculations[19] show that on the dynamical theory under certain conditions Sheckley partial may be invisible even if $\vec{g}.\vec{b} = -\frac{2}{3}$. Another type of partial dislocation which exists in the face centred cubic system is the Frank partial of the type

$\vec{b} = \frac{a}{3}[111]$. In this case also $\vec{g}.\vec{b}$ can take values of $0, \pm\frac{1}{3}, \pm\frac{2}{3}$, etc. The edge partials also are effectively invisible for $\vec{g}.\vec{b} = \pm\frac{1}{3}$.

10.5 Burgers Vector Determination

It has already been discussed earlier that if an image of a defect is to be observed then the defect must be bending the particular set of planes out of their original plane as in Fig. 10.11(a), whereas, if the defect causes a distortion which only shifts the atoms within the planes as in Fig. 10.11(b) the electron beam would not detect any displacement, and an image is not observed - the defect is "out of contrast". Mathematically this "out of contrast" condition for a dislocation can be expressed as $\vec{g}.\vec{b} = 0$. If, therefore, the specimen is changed in orientation until the dislocation becomes invisible with a single strong reflection operating, and $\vec{g}$ is determined from the selected area diffraction pattern, one knows that $\vec{g}$ and $\vec{b}$ are mutually perpendicular. Since the crystal structure of the specimen being studied is usually known, the above criterion is adequate to allow $\vec{b}$ to be determined unambiguously. In general, it is necessary to find another value of $\vec{g}$ which gives invisibility by further tilting the specimen. It then follows that $\vec{b}$ lies along the line of intersection of the two reflecting planes concerned, i.e. mutually perpendicular to the two reciprocal lattice vectors

$\vec{g}_1$ and $\vec{g}_2$. If the two reflecting planes are (h_1,k_1,l_1) and (h_2, k_2, l_2) it follows that

$\mathbf{b} = [uvw]$ is given by

$$[uvw] = [k_1l_2 - l_1k_2,\ l_1h_2 - l_2h_1,\ h_1k_2 - k_1h_2]$$

This provides the direction of the Burgers vector, but not its magnitude. However, the direction is usually sufficient because the magnitude must correspond to a small lattice vector, and this is unique once the direction is known.

10.6 References

1. Hirsch, P. B., Horne, R. W. and Whelan, M. J.
Phil. Mag. 8 (1956) 677.

2. Hirsch, P. B., Howie, A. and Whelan, M. J.
Phil. Trans. Roy. Soc. A 252 (1960) 499.

3. Hirsch, P. B., Howie, A. and Whelan, M. J.
Proc. 4th Inter. Conf. on Electron Microscopy, Berlin, 1 (1960) 527.

4. Bollman, W.
Phys. Rev. 103 (1956) 1588.

5. Amelinckx, S.
Sol. St. Phys. Suppl. 6 (1964).

6. Heidenreich, R. D.
Fundamentals of Transmission Electron Microscopy, Interscience, New York (1964).

7. Hirsch, P. B., Howie, A., Nicholson, R.B., Pashley, D. B. and Whelan, M. J.
Electron Microscopy of Thin Crystals Butterworths, London (1967).

8. Amelinckx, S., Gevers, R., Remaut, G. and Van Landuyt, J.
Modern Diffraction and Imaging Techniques in Materials Science, North Holland, Amsterdam (1970).

9. Murr, L. E.
Electron Optical Applications in Materials Science, McGraw Hill, New York (1971).

10. Valdre, U.
'Electron Microscopy in Materials Science', Academic Press, New York (1971).

11. Whelan, M. J.
Modern Diffraction and Imaging Techniques in Material Science (Eds. Amelinckx, S., Gevers, R., Remaut, G. and Van Landuyt, J) North Holland and Amsterdam (1970), 35.

12. Howie, A.
Electron Microscopy in Materials Science (Ed. Valdre, U.) Academic Press, New York (1971) 274.

13. Howie, A.
Modern Diffraction and Imaging Techniques in Material Science (Eds. Amelinckx, S., Gevers, R., Remaut, G. and Van Landuyt, J.) North Holland, Amsterdam (1970) 295.

14. Goringe, M. J.
Electron Microscopy in Materials Science (Ed. Valdre, U.) Academic Press, New York (1971) 462.

15. Jouffrey, B. and Taupin, D.
Phil. Mag. 16 (1967) 703.

16. Howie, A. and Basinski, Z. S.
Phil. Mag. 17 (1968) 1039.

17. Colliex, C., Jouffrey, B. and Taupin, D.
Phil. Mag. 19 (1969) 873.

18. Howie, A. and Whelan, M. J.
Proc. Roy. Soc. A 267 (1962) 206.

19. Silcock, J. and Tunstall, W. J.
Phil. Mag. 10 (1964) 361.

Captions of the figures

Fig. 10.1 The ray diagram for the objective lens of an electron microscope. The broken lines represent diffracted beams.

Fig. 10.2 Illustrating diffraction contrast for dark field illumination with tilted electron gun.

Fig. 10.3 Illustration of beam for bright field electron microscopy.

Fig. 10.4 Illustration of beam path for dark field electron microscopy.

Fig. 10.5 The column approximation for a perfect crystal.

Fig. 10.6 A series of two-beam diffraction pattern suitable for forming strong images near B = [011] in a f.c.c. crystal structure.

Fig. 10.7 The definition of vectors, s.s, g + s in terms of the Ewald sphere construction in reciprocal space.

Fig. 10.8 The column approximation for a thin foil containing a screw dislocation DD.

Fig. 10.9 s positive with the equivalent positions of the reciprocal lattice point and the Ewald sphere. The bright Kikuchi line is outside it.

Fig. 10.10 Stacking fault running across a foil causing the column to be displaced.

Fig. 10.11 Atomic displacements caused by lattice defects which

(a) distort a set of lattice planes out of their original plane, and

(b) only shift the atoms within the original plane.

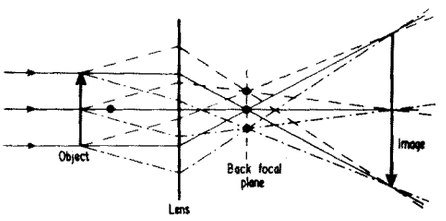

Fig. 10.1

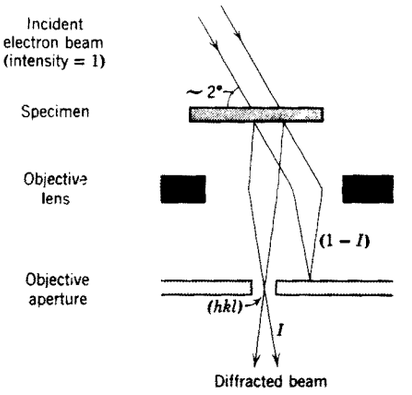

Fig. 10.2

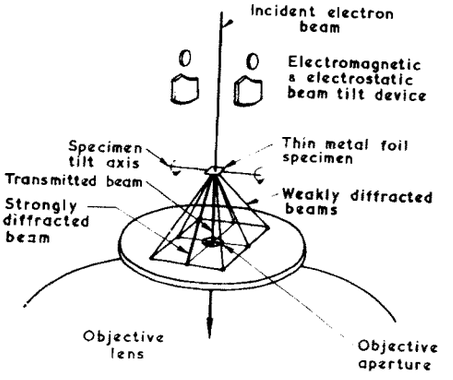

Fig. 10.3

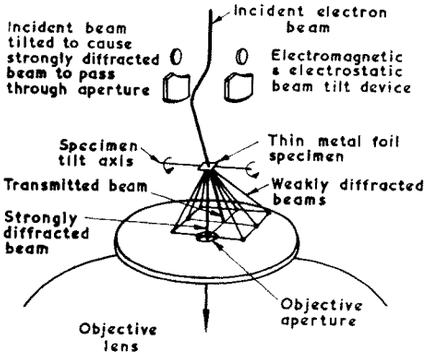

Fig. 10.4

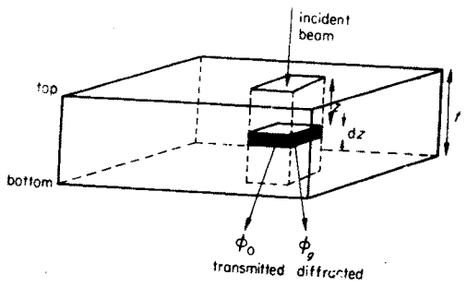

Fig. 10.5

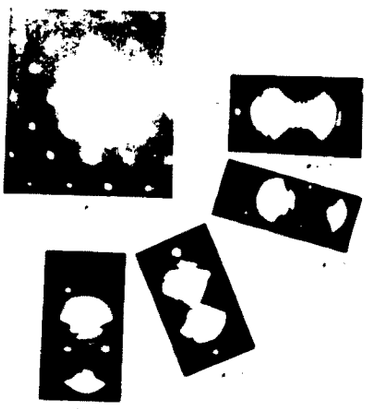

Fig. 10.6

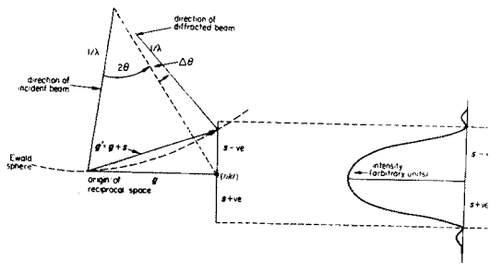

Fig. 10.7

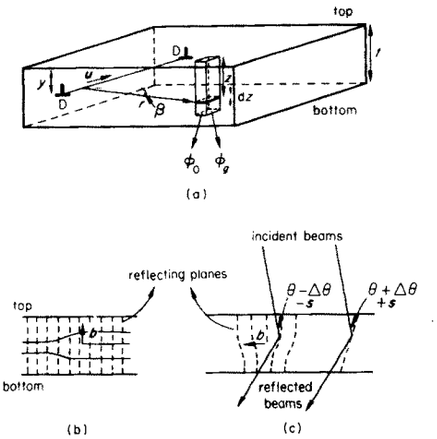

Fig. 10.8(a,b,c)

Fig. 10.9

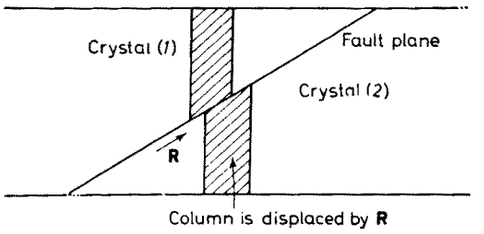

Fig. 10.10

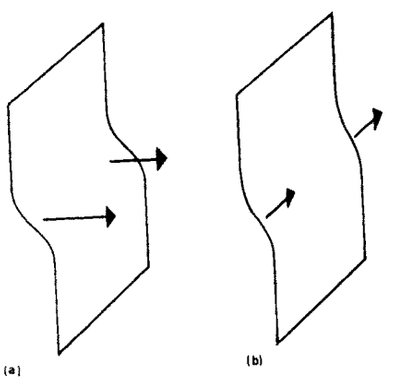

Fig. 10.11